HEWLETT hp PACKARD

COMPONENTS

APPLICATION NOTE 961

Silicon Double-Drift IMPATT Diodes For Pulse Applications

CONTENTS

I. INTRODUCTION

II. MICROWAVE CIRCUITS

- a. Equivalent Circuit
- b. Fixed-tuned Coaxial Cavity

III. MICROWAVE PERFORMANCE

- a. Dependence on Operating Current
- b. Dependence on Operating Frequency
- c. Dependence on Pulse Width and Duty Cycle

IV. INJECTION LOCKING

APPENDIX A – GENERAL PURPOSE PULSE BIAS CIRCUITS

- a. Basic Pulse Amplifier
- b. Fast Risetime Pulse Amplifier
- c. Pulse-DC Adder Circuits

Other relevant HP Application Notes:

AN 935, Microwave Power Generation and Amplification Using IMPATT Diodes – a general introduction to IMPATT diode physics, construction, and operation.

AN 962, Silicon Double-Drift IMPATTs for High-Power CW Applications – presents a more in-depth discussion of the double-drift IMPATT diode structure and characteristics, including impedance and noise properties.

AN 959-1, Factors Affecting Silicon IMPATT Diode Reliability and Safe Operation – a short note on how to keep an IMPATT diode alive.

AN 959-2, Reliability of Silicon IMPATT Diodes – a short note discussing both theoretical and observed failure rates in silicon IMPATT diodes.

INTRODUCTION

In recent years the silicon IMPATT diode has proven to be a practical, easy to use and reliable solid-state source of microwave and millimeter-wave power[1]. Hewlett-Packard has developed double-drift[2] IMPATT devices for the efficient generation of high average power and high peak power between 8 and 18 GHz[3]. A graphic illustration of the capabilities of these devices is given in Figure 1 which shows the RF spectrum of a typical 10.5 GHz diode delivering 14 watts of microwave power at 11.5% efficiency with a duty cycle of 25%.

The basic structure of the P^+PNN^+ double-drift-region IMPATT diode is illustrated in Figure 2. The structure of the more familiar P^+NN^+ single-drift-region IMPATT diode is shown for comparison. In both devices the active region is sandwiched between highly doped P^+ and N^+ contacting layers. The double-drift structure has two moderately doped central regions rather than one, so that the electric field profile in the depletion zone is nearly symmetrical about the PN junction.

When either of these devices is reverse biased into avalanche breakdown, electrons and holes are generated in an avalanche zone near the peak electric field. In the single-drift IMPATT diode, the holes generated in the avalanche zone are immediately collected by the P^+ contact and do not contribute to the transit-time negative resistance. In the double-drift IMPATT diode, both the electrons and holes experience a transit-time delay in their respective drift regions after leaving the central avalanche zone. Both contribute to the transit-time negative resistance.

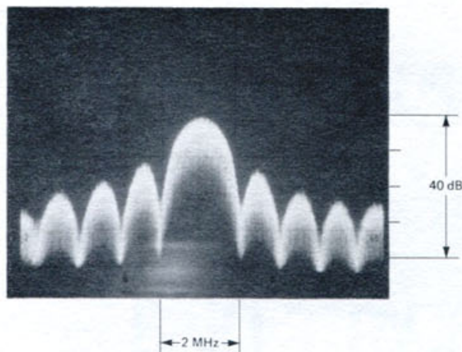

(a.) Logarithmic pulse spectrum.

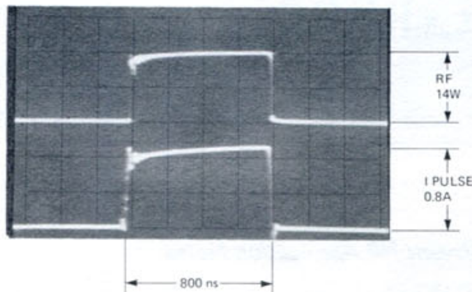

(b.) Detected RF output and bias current pulse.

Figure 1. Typical pulsed performance at 10 GHz and 25% duty cycle.

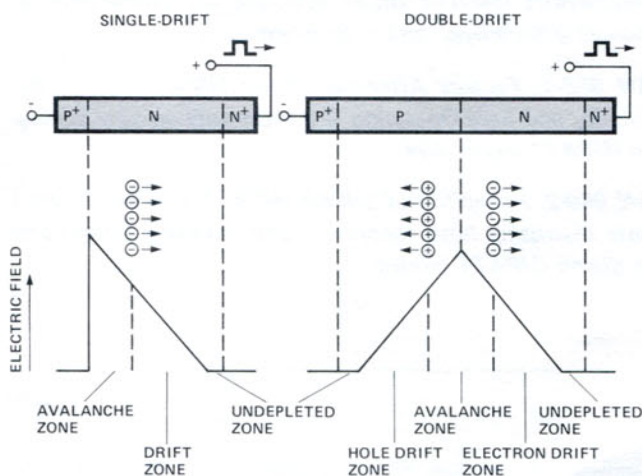

Figure 2. Comparison of single-drift double-drift IMPATTs. The electric field profile at breakdown is shown.

The end result of both carrier types contributing to the negative resistance is that a double-drift device is superior to a comparable single-drift device of the same area in terms of efficiency, power output and noise. Even larger power outputs are possible from double-drift IMPATT diodes than from single-drift diodes since larger area devices can be fabricated and easily resonated due to the smaller capacitance per unit area. This advantage is particularly significant for pulsed devices where thermal limitations do not restrict operation to low current densities.

MICROWAVE CIRCUITS

Double-drift IMPATT diodes are fabricated using an integral plated heatsink process. The individual chips are bonded into a ceramic microwave package designed particularly for large area diodes with high values of junction capacitance at breakdown. A cross section of the stud package is shown in Figure 3. This package is distinguished from more commonly used ceramic microwave packages by a lower ceramic height, resulting in less parasitic inductance and a consequent improvement in the ease of resonating high capacitance devices at X- and Ku-band frequencies.

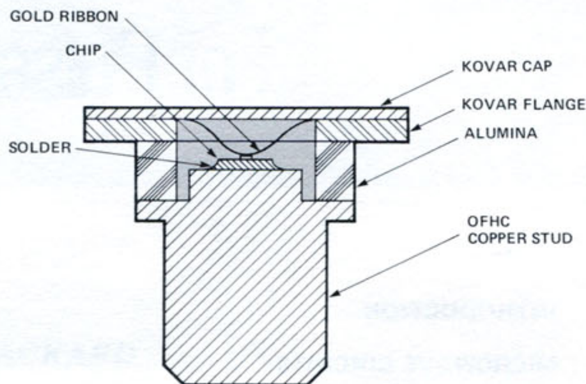

Figure 3. Cross section of IMPATT diode chip in style 46 package.

Equivalent Circuit

A simple lumped element equivalent circuit for a chip mounted in a style 46 package is shown in Figure 4.

The four-element equivalent circuit for the package consists of two inductors and two capacitors whose values are frequency independent. The capacitance C_p resides mainly in the ceramic dielectric, while the capacitance C_m results from the shunt capacitance between the gold contacting mesh and the package stud. L_2 corresponds to the inductance of the contacting mesh, and L_1 may be thought of as an external inductance arising from the magnetic energy stored in the cylindrical region around the package.

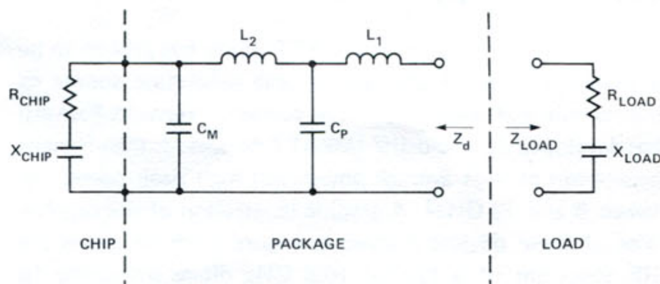

PACKAGE 46 (NO RECESS)		
PARAMETER	DESCRIPTION	TYPICAL VALUE
L_1	EXTERNAL INDUCTANCE	0.26 nH (MOUNT – DEPENDENT)
L_2	MESH INDUCTANCE	0.15 nH
C_p	PACKAGE CAPACITANCE	0.55 pF (CAN VARY FROM 0.4 TO 0.6 pF)
C_M	MESH CAPACITANCE	0.05 pF

Figure 4. Equivalent circuit of packaged IMPATT diode chip.

Because of its origin, L_1 is highly dependent on the mounting arrangement. With proper values for C_p, C_m, L_1, and L_2 it has been found that this equivalent circuit can accurately model the style 46 package to frequencies up to 18 GHz.

Representative values for the elements in the package equivalent circuit are listed in Figure 4 for the special case where the package is not recessed into the shorting plane of the cavity. Recessing the package is a useful technique for reducing L_1 and thus making it easier to resonate the diode at high frequencies. The specific values listed in Figure 4 were determined using an automatic network analyzer in a manner similar to that described by Monroe[4].

The impedance of the chip, $R_{chip} + j\ X_{chip}$, is highly dependent on the bias current, frequency of operation and RF voltage modulation. The chip resistance can be negative over a frequency range greater than 1.5 octaves. Within this active frequency range the chip reactance, X_{chip}, is capacitive except near the lower limit of negative resistance where X_{chip} can become inductive.

A double-drift IMPATT diode can operate either as an amplifier or an oscillator, depending on the loading. The real and imaginary parts of the load impedance, Z_{load}, are the variables whose values determine the mode of operation. The diode can function as an amplifier if the load resistance presented to it at the resonant frequency is larger in magnitude than the diode's negative resistance. For an amplifier using X- or Ku-band double-drift diodes R_{load} will typically be greater than 5 ohms. The load reactance, X_{load}, required to resonate the diode can be either capacitive or inductive depending on the package mounting arrangement and the operating frequency.

The diode functions as an oscillator when Z_{load} is the negative of the diode impedance. In this mode R_{load} is typically between 0.5 and 2.5Ω, as shown in Figures 8 and 9.

Fixed-Tuned Coaxial Cavity

The cross section of a simple coaxial cavity that has been found particularly well suited for pulsed double-drift IMPATTs operated at frequencies up to 18 GHz is shown in Figure 5. The transformation from the 50 ohm transmission line to the diode impedance is accomplished by a Rexolite-loaded low impedance transmission line section with a characteristic impedance of Z_o.

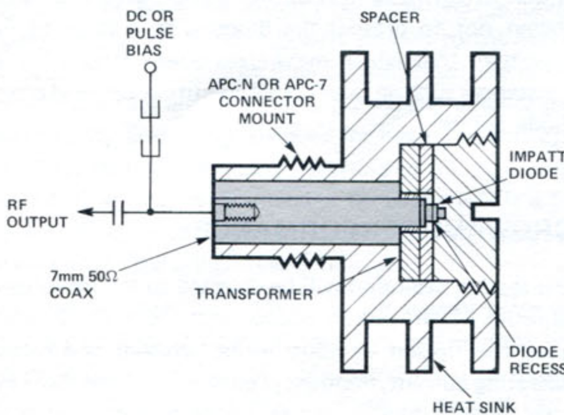

Figure 5. Cross section of low parasitic fixed-tuned coaxial cavity.

The resonant frequency of a diode in this cavity can be adjusted by changing the thickness of the spacer behind the transformer, the electrical length of the transformer section, or the depth of diode recess. Typical examples of the shifts in resonant frequency that can be accomplished by reducing the diode inductance through recessing the package are illustrated in Figure 6 for both the X- and Ku-band devices. No spacers were used in either case. Capacitive loading was achieved by using transformers whose electrical lengths were approximately 1/8 λ.

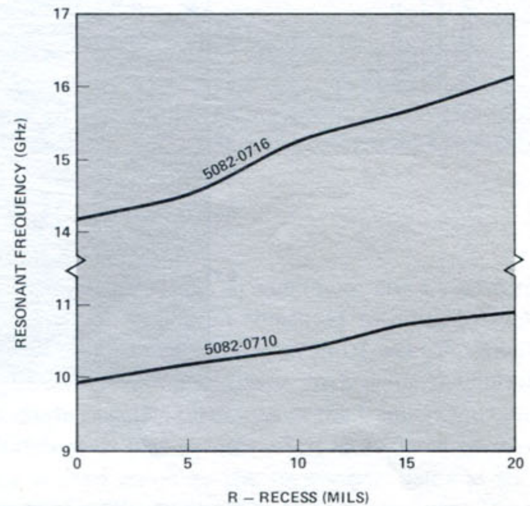

Figure 6. Influence of package recess depth on operating frequency.

Figure 7(a) is a graphical aid to the determination of the proper Z_o and length of the transformer. Two examples using the 5082-0710 serve to illustrate its use. Figure 9 shows that the desired load impedance at 9 GHz is 1.8 - j5. Figure 7(a) shows that an 8 ohm transformer of length .16 λ will provide this impedance. At higher frequencies this technique shows that shorter transformers are necessary. For example at 11 GHz the required load impedance is 1.3 - j14, corresponding to a transformer length much less than .1 λ. However, R_{load} changes rapidly with ℓ for ℓ less than λ/8 while R_{load} is insensitive to ℓ for longer transformers. Therefore it is wise to use a λ/8 transformer of proper Z_o to provide the correct R_{load} with the appropriate changes in diode recess or spacer dimensions to provide the correct matching reactance. In this case, a 5.7 ohm λ/8 transformer will provide a load impedance of 1.3 - j5.5. This load would cause the diode to oscillate below the desired 11 GHz frequency. The frequency may be increased to the desired value by recessing the diode or by choosing the proper spacer. Figure 7(b) is included to help the designer to graphically find b/a for the transformer Z_o determined from Figure 7(a).

Figure 7(a). Load resistance versus electrical length of single-step transformer in 50 ohm transmission line. Dashed lines correspond to equal load reactance for different values of Z_O.

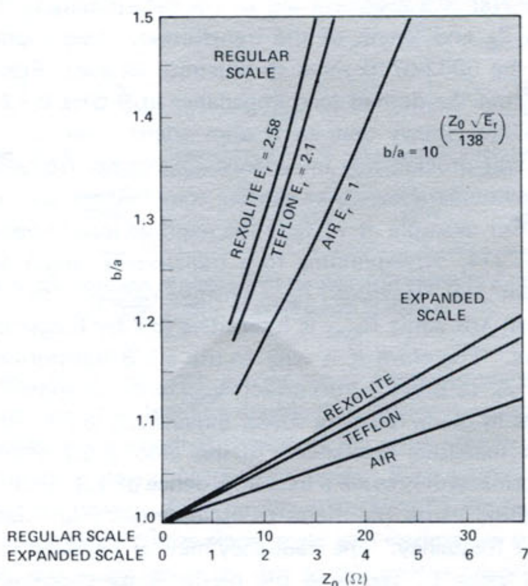

Figure 7(b). b/a versus Z_O.

For optimization of oscillator output power it is often desirable to have continuous control over R_{load}. This control can easily be accomplished by positioning a tuning screw at the proper distance from the diode. This position is best found empirically by having 3 positions available near the diode, spaced λ/8 apart. In this case the value of b/a should be such that R_{load} with the tuning screw removed is greater than that which maximizes output power. Great care should be taken not to present the diode with a value of R_{load} smaller than that which maximizes power output. In certain instances such an overloaded condition can lead directly to diode failure.

MICROWAVE PERFORMANCE

In this section attention will be directed to the performance capabilities of HP pulsed double-drift IMPATT diodes. A detailed description of basic device behavior as a function of operating current, frequency, pulse width, and duty cycle will be given. The important dc parameters and typical microwave performance of diodes designed for X- and Ku-band operation are summarized in Table 1.

Table 1. Typical Pulsed Double-Drift IMPATT Diodes.

Parameter	Symbol	Frequency	
		10.5 GHz (5082-0710)	16.5 GHz (5082-0716)
Peak Output Power	P_O	14W	11W
Efficiency	η	12%	11.5%
Bias Current	I_{OP}	0.81 A	0.9 A
Oscillation Threshold Current	I_{Th}	270mA	300mA
Bias Voltage	V_{OP}	148V	100V
Breakdown Voltage	V_{BR}	115V	78V
Junction Capacitance at Breakdown	$C_j(V_{BR})$	1.25 pF	0.8 pF
Thermal Impedance	Θ_T	6.5°C/W	8.5°C/W
Pulse Width	T_P	800 nsec	800 nsec
Duty Cycle	du	25%	25%
Average Junction Temperature Rise	$\Delta T_{j(avg)}$	⩽175°C	⩽175°C
Temperature Coefficient of Breakdown Voltage	V_b'	0.135V/°C	0.091V/°C
Space Charge Resistance	R_{SC}	11Ω	10.5Ω

In all cases, the diodes were biased by adding an amplified pulse voltage to a fixed dc bias voltage. Appendix A describes general purpose current pulse amplifier and adder circuits appropriate for double-drift IMPATT diodes.

Dependence on Operating Current

For any particular operating frequency the obtainable output power, efficiency, and junction temperature rise are determined mainly by the diode operating current. Curves illustrating the typical behavior of the X- and Ku-band diodes operated near the center of their useful frequency range at a pulse width of 800 nsec and a duty cycle of 25% are shown in Figure 8. The curves were obtained by resonating the diode at the desired frequency and then adjusting the load resistance to maximize the output power at each setting of the bias current.

There are two limitations on bias current: reliability and device stability. Both the output power and average junction temperature rise are almost linearly related to the bias current. Junction temperature directly influences the intrinsic device failure rate and as a consequence the operating current is usually limited by the need for highly reliable operation. Bias currents normally resulting in $\Delta T_{j(avg)}$ greater than 200°C are not recommended because there is a tendency for these diodes to become unstable and noisy when operated under these high bias conditions.

The curves of conversion efficiency are steeply rising functions of operating current at low bias and exhibit broad maxima in excess of 10% at higher currents. It is thus possible to obtain good conversion efficiency even at low operating currents.

Measurements of the large-signal diode negative resistance, and thus load resistance, at maximum output power were made using the oscillation threshold technique developed for IMPATT diodes by van Iperan and Tjassens[5]. This technique involves making accurate small-signal measurements of the diode negative resistance at the frequency of interest as a function of bias current. The large-signal negative resistance is then equal to the small-signal value at the bias current where the diode first starts to oscillate. Changing the circuit load resistance will change the negative resistance of an oscillating diode by forcing a change in the RF diode voltage. Typical curves of diode negative resistance corresponding to maximum output power are shown in Figure 8(d) as a function of operating current. An alternative, but less accurate technique for determining the diode negative resistance is to simply calculate the load resistance presented by the coaxial transformer. The load resistance can be obtained by interpolation of the curves given in Figure 7. In normal operation the circuit load resistance is adjusted to result in maximum output power at a bias current corresponding to a maximum allowed junction temperature rise. The dotted curves in Figure 8(a) illustrate the typical power output versus current characteristics that result if the load resistance is kept fixed at the optimum value for maximum power. In this case the threshold of oscillation occurs exactly at the bias current where the small-signal diode negative resistance equals the load resistance. The threshold bias current for a particular operating frequency is thus an excellent indicator of whether or not the diode is properly loaded. Reduced output power will result if the threshold current is higher than that which corresponds to maximum power output. If the threshold current is less than the optimum value the diode will be in danger of burnout when biased to normal operating currents. The threshold bias current is typically 1/3 of the normal operating current.

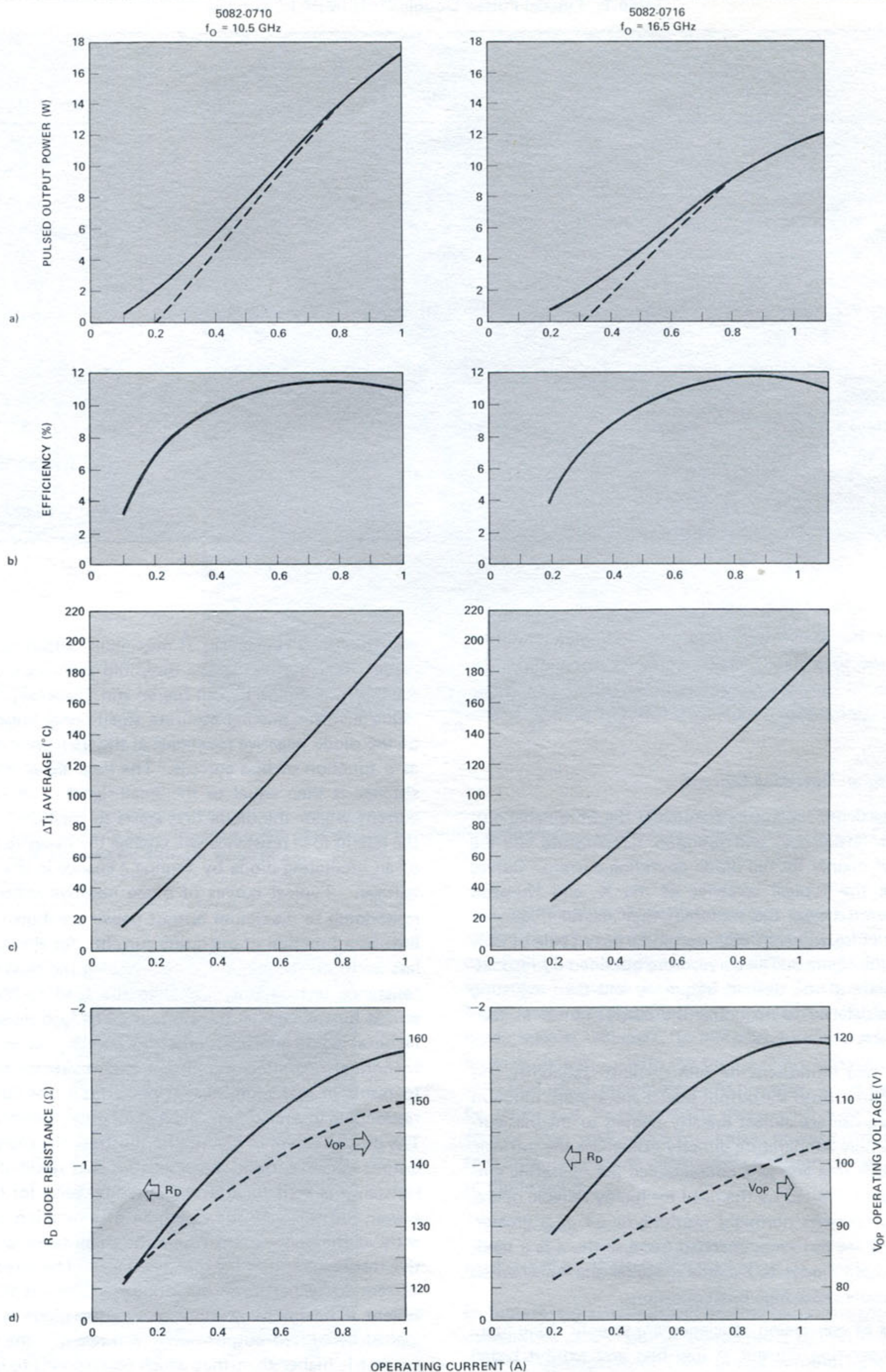

Figure 8. Influence of operating current on maximum available output power, efficiency, average junction temperature rise, large-signal diode resistance and operating voltage of typical diodes at 800 nsec pulse width and 25% duty cycle. Dotted curve of power output versus current corresponds to fixed circuit tuned to result in maximum output power at a bias current of 0.81 amps for 5082-0710 and 0.9 amps for 5082-0716.

Dependence on Operating Frequency

Double-drift IMPATT diodes can exhibit small-signal negative resistances over a greater than 1.5 octave frequency range. They are capable of generating near maximum output power over a significant fraction of this range. The wide frequency range of useful power output is illustrated in Figure 9 for both the X- and Ku-band devices. The two devices can easily be tuned over the entire X- and Ku-bands respectively. Pulsed output powers greater than 12 watts in X-band and 9 watts in Ku-band can be obtained over a 4 GHz frequency range in both bands with efficiencies between 10 and 12%.

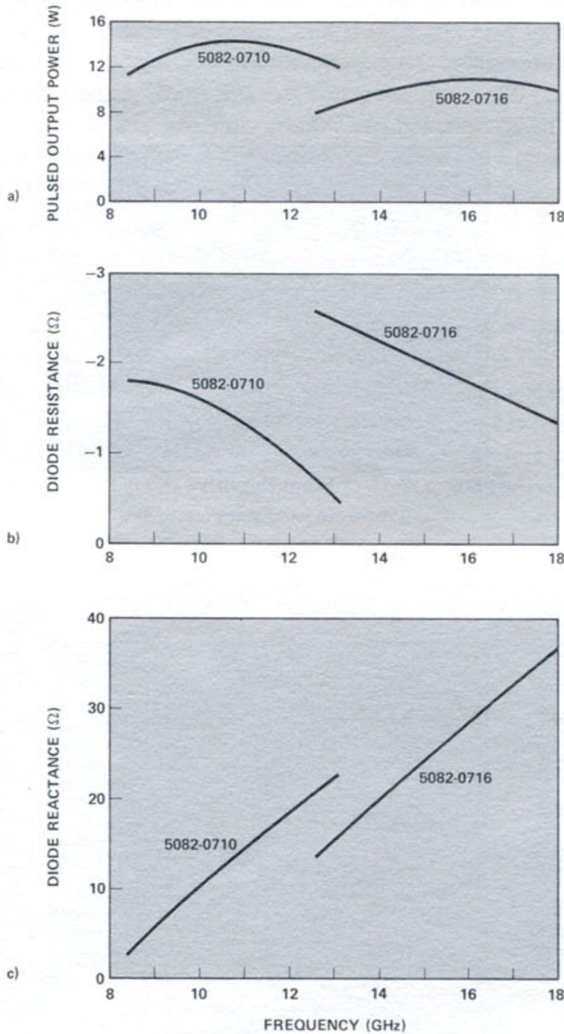

Figure 9. Influence of operating frequency on maximum output power and optimum diode negative resistance for $\Delta T_{j(avg)} \leq 175^\circ C$. Diode reactance is represented by small-signal values measured at a bias current of 300mA.

The load resistance was adjusted for maximum output power at each operating frequency and the large-signal diode resistance was inferred using the oscillation threshold technique described above. The results shown in Figure 9 reveal a negative diode resistance that decreases monotonically with frequency.

The small-signal diode reactances for a dc bias current of 300mA are also plotted in Figure 9 as a function of frequency. These values approximate the large-signal diode reactances. The curves correspond to the case of zero package recess. They are included here for illustrative purposes in order to give an indication of the magnitude of the diode inductive reactance which must be resonated.

Dependence on Pulse Width and Duty Cycle

All of the discussion so far has been concerned with operation at 800 nsec pulse width and 25% duty cycle. Many applications of pulsed double-drift diodes will have other pulse width and duty cycle requirements. The output power capabilities of both devices were therefore determined over the range of pulse widths from 0.1 µsec to 50 µsec with the only limitation being that the junction temperature rise be less than 200°C. Measurements were made for duty cycles of 1, 10, and 25%. The results for operation at 10.5 and 16.5 GHz are illustrated in Figure 10.

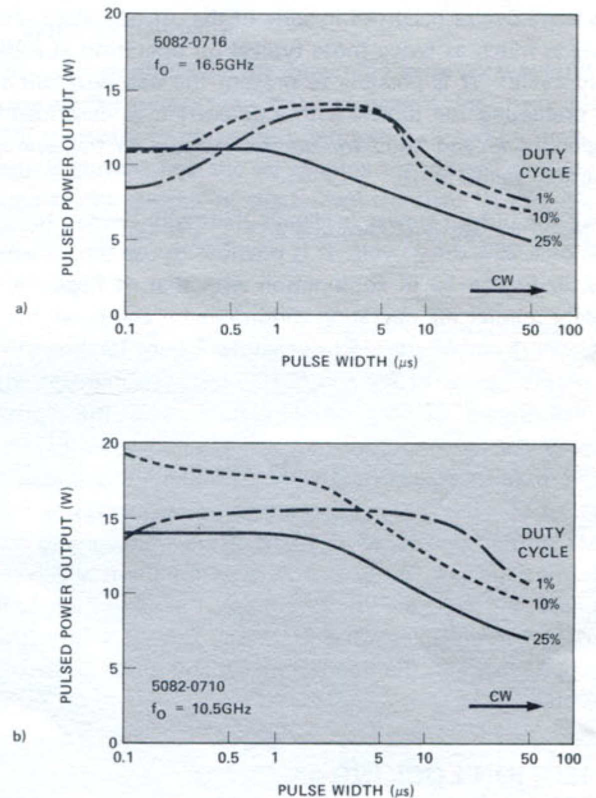

Figure 10. Influence of pulse width on maximum output power of typical X- and Ku-band diodes operated at duty cycles of 1, 10, and 25% with $\Delta T_j \leq 200^\circ C$.

For pulse widths greater than 10 µsec the output power is limited only by the restriction that ΔT_j be less than 200°C. Output power therefore decreases smoothly with either increasing pulse width or duty cycle. For pulse widths less than 5 µsec, however, electronic limitations complicate the observed device behavior. This is particularly true for very

short pulses and low duty cycles where the average junction temperature rise is minimal. The electronic limitations are more severe for the 16.5 GHz device than for the more thermally limited 10.5 GHz device.

A decrease in average junction temperature can, in fact, have a detrimental effect on output power and efficiency. This decrease results in part from an increase in series loss in the undepleted portions of the N and P layer due to the reduction in the width of the depleted region at lower temperature. In addition, the frequency at which maximum power can be obtained is inversely dependent on junction temperature. Some of the reduction in obtainable output power at low duty cycles and short pulses can therefore be attributed to an upward shift in the optimum frequency away from the 10.5 and 16.5 GHz operating frequencies. A third effect which can decrease the peak output power as the average temperature decreases stems from a corresponding decrease in the RF voltage amplitude. The maximum RF voltage amplitude in IMPATT diodes is limited to a fixed fraction of the dc bias voltage, and this decreases with decreasing junction temperature.

The observed roll off in performance for short pulses and low duty cycles occurred in spite of the use of current densities as much as twice those typical for operation at a 25% duty cycle. It is possible to prevent the observed roll off by prebiasing the diodes with a dc current as described in Appendix A and thus forcing an increase in the average junction temperature.

Since the output power is always thermally limited for the case of a 25% duty cycle, it is possible to use the information in Figure 10 in conjunction with that of Figure 8 to closely predict the operating conditions for any pulse width between .1 and 50 μsec. For example, Figure 10 shows that an output power of 7 watts at 10.5 GHz is obtainable with a pulse width of 50 μsec, while Figure 8 reveals the approximate operating conditions required. In particular, Figure 8 shows that an operating current of 480mA and a load resistance of -1.1 ohms will result in an output power of 7 watts with an efficiency of 10.6%. It is interesting to note that the efficiency is above 10% even for the low currents required for the case of long pulses. If operation is required at frequencies other than 10.5 and 16.5 GHz, then Figure 9 illustrates the trend of power and diode impedance expected.

INJECTION LOCKING

For reasons of noise, stability or precise frequency control, it is often necessary that an oscillator be injection locked to an external signal. The phase locking of pulsed double-drift IMPATTs operated in the simple coaxial cavity described above is easily accomplished by coupling the injected signal to the oscillator through a broadband coaxial circulator.

Typical locking characteristics for the HP 5082-0716 and 0710 are illustrated in Figure 11. In both cases, the load resistances were initially tuned to result in a maximum free-running oscillator output power. The resulting curves of locking gain versus frequency are nearly symmetrical about the center oscillator frequency f_o. The indicated values of locking Q, Q'_{ext}, for the HP 5082-0716 and 0710 were 33 and 19 respectively. For a locking gain of 10 dB, it is apparent that both devices could be locked over a bandwidth of approximately 400 MHz.

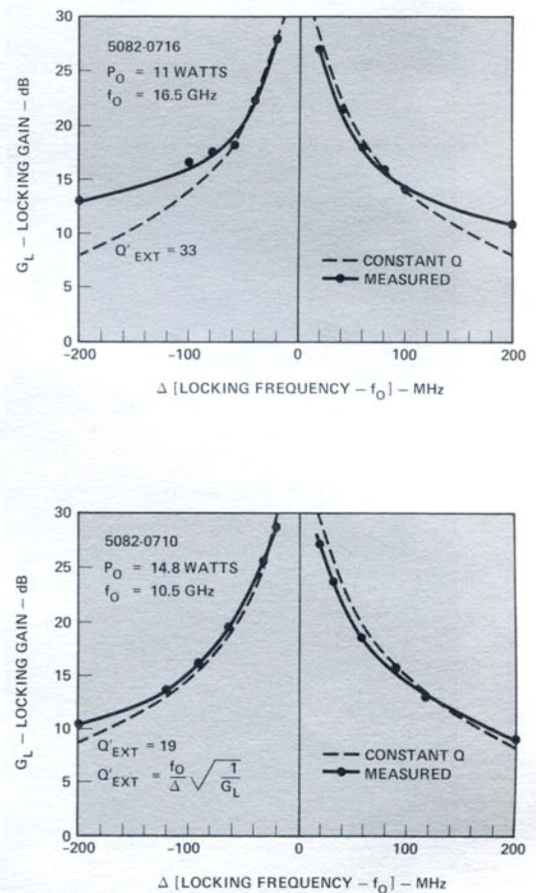

Figure 11. Typical locking characteristics of X- and Ku-band diodes.

APPENDIX A

GENERAL PURPOSE PULSED BIAS CIRCUITS

The wide variety of possible pulsed applications requires bias sources with different risetime, pulse width and duty cycle capabilities. Ideally a bias supply optimized for each application should be designed. In many cases, however, a general purpose pulse supply is adequate for early investigations and prototype development. This appendix describes pulse amplifier and adder circuits that meet the general requirements presented by pulsed silicon double-drift IMPATTs.

Any pulser designed specifically for IMPATTs must be able to accommodate the approximately 1% increase in breakdown voltage that occurs for every 10°C temperature rise during a pulse. Conventional voltage source or 50 ohm impedance pulsers are not suitable, in general. With these pulsers the RF output power will typically show a characteristic droop with time, as the diode current decreases.

On the other hand, a current source pulser can be built which will supply a constant current during the pulse in spite of the changing voltage across its load. In this case, the RF output will be nearly flat, with a gradual increase in power during the pulse due to junction heating. For those applications requiring a minimum of chirp, (sin x)/x spectra can be obtained if the current is allowed to increase slightly (5-20%) during the pulse. The spectrum shown in Figure 1 was obtained from a diode biased in such a manner.

The block diagram of a general purpose pulse bias current source for IMPATTs is shown in Figure A1. The basic elements are a pulse amplifier and an adder, both of which are described in the following sections.

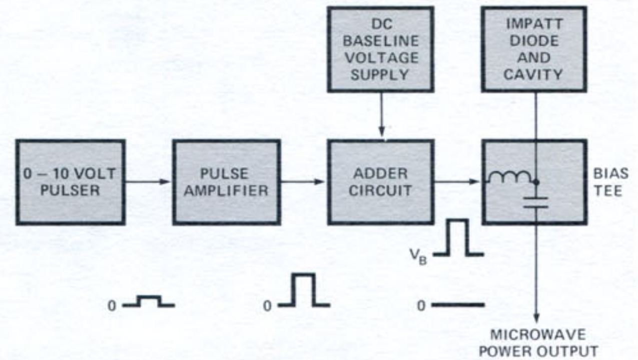

Figure A1. Block diagram of bias circuitry for pulsed operation of double-drift IMPATTs.

a. Basic Pulse Amplifier

The pulse amplifier circuit shown in Figure A2 was built for pulse widths greater than 200 nsec using a slow, high voltage PNP transistor in the output. Inductors L_1 and L_2 shape the output current risetime by shaping the voltage risetime applied to the emitter of the output transistor(s) through the limiting resistor $R_{2a \to j}$. The common base output transistor

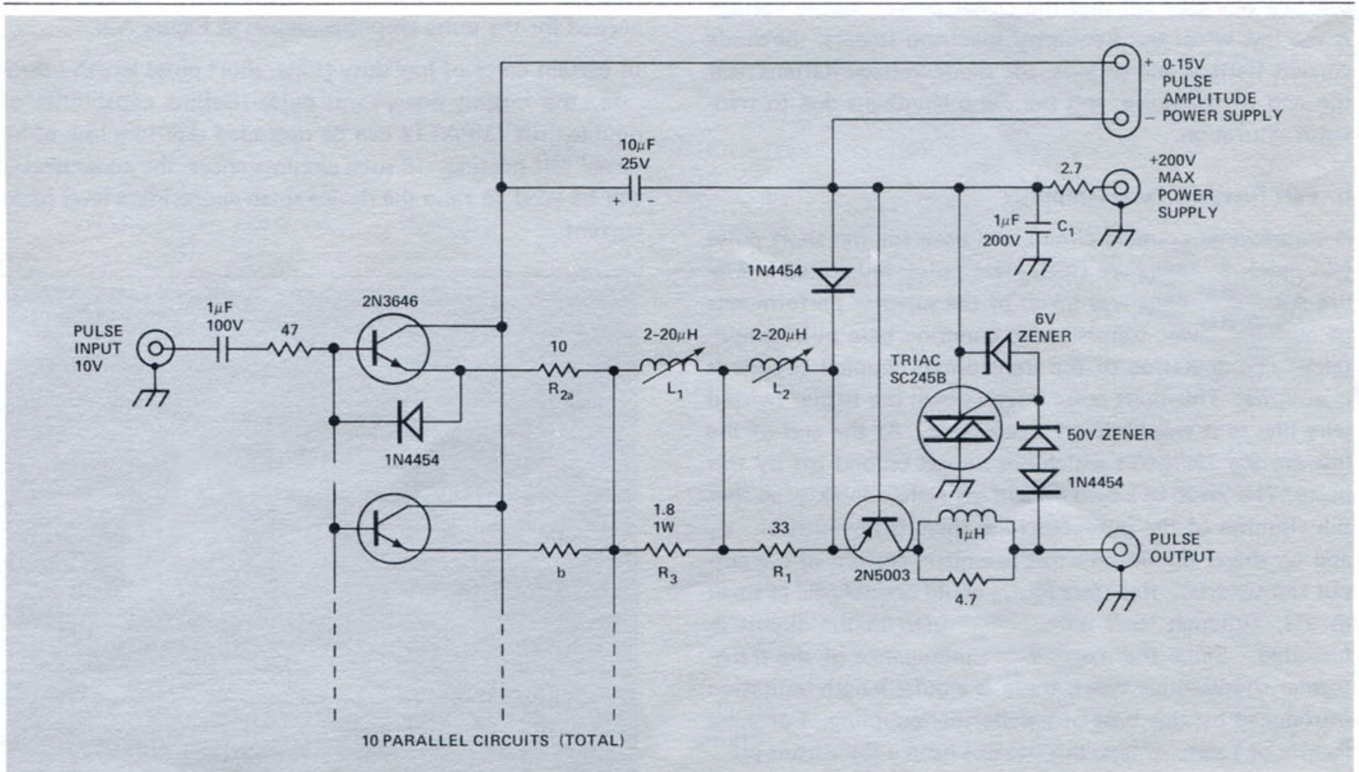

Figure A2. Circuit of pulse amplifier suitable for pulse lengths between 0.2 and 50 µsec. Increase C_1 for pulses longer than 10 µsec. The Triac acts as a crowbar, putting a short circuit across the 2N5003 transistor when the voltage exceeds 55V.

Figure A3. Circuit of fast risetime pulse amplifier suitable for pulse lengths between .05 and 1 μsec.

is a reasonable current source so long as it is not permitted to saturate. Therefore at the end of the pulse a few volts should remain from the collector to base. At the beginning of the pulse the output transistor has to drop considerably more voltage. Clearly, all of the IMPATT diode voltage change has to be absorbed by the output transistor. In practice one can tell that the pulser power supply voltage is too low when the frequency spectrum smears, the diode current flattens and droops, the diode voltage flattens near the end of the pulse, and the pulse lengthens due to transistor saturation.

b. Fast Risetime Pulse Amplifier

A transformer coupled circuit was used for the short pulse (<1 μsec), fast risetime (<10 nsec) pulser illustrated in Figure A3. Advantage was taken of the superior performance of NPN rf power transistors as common base pulse amplifiers. The operation of the transformer coupled circuits is as follows: The input pulse travels down the trifilar twisted wire line as it would down a coax line. At the end of the line are the 2N3646's which are turned on and off by this pulse. The 2N3646's turn on and off rather quickly, so that the risetime of the pulse reaching them is not critical. L_1 and L_2 shape the risetime of the emitter current of the output transistor(s). Resistors $R_{2a\rightarrow d}$ could possibly be as small as 2Ω, although larger values were used in the circuit illustrated. Since the magnetizing inductance of the transformer shunts the output, there is a pulse length limitation introduced by this type of transformer coupling. For pulse lengths of 1 μsec or less, this has not been a significant problem since more slope could easily be added to the output transistors to compensate for the output current lost due to the magnetizing current.

c. Pulse-DC Adder Circuit

Under normal high duty cycle operation the adder circuit shown in Figure A4 is used to raise the baseline dc voltage to a level slightly less than the IMPATT diode breakdown voltage. Only in this manner can the current-source pulse amplifier above be utilized effectively. This circuit is not needed for the pulse amplifier shown in Figure A2.

In certain cases of low duty cycle, short pulse length operation, the output power and pulse risetime capabilities of double-drift IMPATTs can be degraded due to a lack of internal self heating. In such circumstances, the adder circuit can be used to raise the device to an appropriate level of dc current.

Figure A4. DC and pulse bias adder circuit.

REFERENCES

1. S. M. Sze and R. R. Ryder, "Microwave Avalanche Diodes," Proc. IEEE (Special Issue on Microwave Semiconductors), 50, pp. 1140-1154, Aug. 1971.
2. D. L. Scharfetter, W. J. Evans, and R. L. Johnston, "Double-Drift-Region (P^+PNN^+) Avalanche Diode Oscillators," Proc. IEEE (lett.), 58, pp. 1131-1133, 1970.
3. G. Pfund, A. Podell, and U. Tarakci, "Pulsed Silicon Double-Drift IMPATTs for Microwave and Millimeter-Wave Applications," Electron. Lett., 9, Nov. 1, 1973.
4. J. Monroe, "The Effect of Package Parasitics on the Stability of Microwave Negative Resistance Devices," IEEE Trans. Microwave Theory Tech., MTT-21, pp. 731-735, Nov. 1973.
5. B. B. van Iperan and H. Tjassens, "Novel and Accurate Methods for Measuring Small-Signal and Large-Signal Impedances of IMPATT Diodes," Philips Res. Repts., 27, pp. 38-75, 1972.

Hewlett Packard assumes no responsibility for the use of any circuits described herein and makes no representations or warranties, express or implied, that such circuits are free from patent infringement.

For more information, call your local HP Sales Office or East (301) 948-6370 - Midwest (312) 677-0400 - South (404) 434-4000 - West (213) 877-1282. Or write: Hewlett-Packard Components, 640 Page Mill Road, Palo Alto, California 94304. In Europe, Post Office Box 85, CH-1217, Meyrin 2, Geneva, Switzerland. In Japan, YHP, 1-59-1, Yoyogi, Shibuya-Ku, Tokyo, 151.

Printed in U.S.A. Revised from 5952-0497(11/74) — Data Subject to Change 5952-8467 (2/76)